

AD-756 890

TRANSITION RUN-OUT CALCULATIONS FOR A
COMPRESSIBLE BOUNDARY LAYER WITH WALL
COOLING

John E. Yates, et al

Aeronautical Research Associates of Princeton,
Incorporated

Prepared for:

Air Force Flight Dynamics Laboratory

October 1972

DISTRIBUTED BY:

NTIS

National Technical Information Service
U. S. DEPARTMENT OF COMMERCE
5285 Port Royal Road, Springfield Va. 22151

AFFDL-TR-72-123

AD756890

**TRANSITION RUN-OUT CALCULATIONS
FOR A COMPRESSIBLE BOUNDARY LAYER
WITH WALL COOLING**

*JOHN E. YATES
COLEMAN duP. DONALDSON*

AERONAUTICAL RESEARCH ASSOCIATES OF PRINCETON, INC.

TECHNICAL REPORT AFFDL-TR-72-123

OCTOBER 1972

Reproduced by
NATIONAL TECHNICAL
INFORMATION SERVICE
U S Department of Commerce
Springfield VA 22151

Approved for public release; distribution unlimited.



**AIR FORCE FLIGHT DYNAMICS LABORATORY
AIR FORCE SYSTEMS COMMAND
WRIGHT-PATTERSON AIR FORCE BASE, OHIO**

NOTICE

When Government drawings, specifications, or other data are used for any purpose other than in connection with a definitely related Government procurement operation, the United States Government thereby incurs no responsibility nor any obligation whatsoever; and the fact that the government may have formulated, furnished, or in any way supplied the said drawings, specifications, or other data, is not to be regarded by implication or otherwise as in any manner licensing the holder or any other person or corporation, or conveying any rights or permission to manufacture, use, or sell any patented invention that may in any way be related thereto.

ACCESSION for		
NTIS	White Section	<input checked="" type="checkbox"/>
B/C	Buff Section	<input checked="" type="checkbox"/>
UNANNOUNCED		<input type="checkbox"/>
JUSTIFICATION		
BY		
DISTRIBUTION/AVAILABILITY CODES		
Dist.	AVAIL. and/or	SPECIAL
A		

Copies of this report should not be returned unless return is required by security considerations, contractual obligations, or notice on a specific document.

UNCLASSIFIED

Security Classification

DOCUMENT CONTROL DATA - R & D

(Security classification of title, body of abstract and indexing annotation must be entered when the overall report is classified)

1. ORIGINATING ACTIVITY (Corporate author) Aeronautical Research Associates of Princeton, Inc. 50 Washington Road, Princeton, NJ 08540	2a. REPORT SECURITY CLASSIFICATION N/A
	2b. GROUP

3. REPORT TITLE
Transition Run-Out Calculations for a Compressible Boundary Layer with Wall Cooling

4. DESCRIPTIVE NOTES (Type of report and inclusive dates)
Final Report; January 1972 - October 1972

5. AUTHOR(S) (First name, middle initial, last name)
John E. Yates
Coleman duP. Donaldson

6. REPORT DATE December 1972	7a. TOTAL NO. OF PAGES 38 42	7b. NO. OF REFS 20
---------------------------------	---------------------------------	-----------------------

8a. CONTRACT OR GRANT NO. F33615-72-C-1350	9a. ORIGINATOR'S REPORT NUMBER(S) A.R.A.P. Report No. 183
b. PROJECT NO. 1366	

c. Task No. 136606	9b. OTHER REPORT NO(S) (Any other numbers that may be assigned this report) AFFDL-TR-72-123
--------------------	------------------------------------------------------------------------------------------------

10. DISTRIBUTION STATEMENT
Approved for public release; distribution unlimited

11. SUPPLEMENTARY NOTES	12. SPONSORING MILITARY ACTIVITY Air Force Flight Dynamics Laboratory Air Force Systems Command Wright-Patterson AFB, Ohio 45433
-------------------------	-------------------------------------------------------------------------------------------------------------------------------------------

13. ABSTRACT
The analytic model developed in AFFDL-TR-70-153 (Ref. 1) for the study of transition in a compressible boundary layer is used to make comprehensive transition run-out calculations for Mach numbers between 0 and 12 and wall temperature ratios between 0.05 and 1.2. Calculated results for the transition Reynolds number and the minimum critical Reynolds number for a growing boundary layer are compared with previous calculations for a frozen uniform parallel flow and with experimental transition results. It is shown that increasing Mach number has a strong favorable effect on the transition Reynolds number, while wall cooling has an adverse effect. Minimum critical Reynolds numbers calculated for a growing boundary layer are larger than those for a frozen parallel flow, in particular at higher Mach numbers. It is also found that wall cooling has an adverse effect on growing mode minimum critical R_x , while it has a favorable effect on the frozen mode minimum critical. The order of magnitude and Mach number trend of the theoretical results are in agreement with experiment. Also the theory predicts the beginning of transition at the outer edge of the boundary layer for hypersonic Mach numbers, in complete agreement with experimental findings of Beckwith and Bertram, NASA TM X-2566 (Ref. 18).

DD FORM 1473
1 NOV 65

UNCLASSIFIED
Security Classification

**TRANSITION RUN-OUT CALCULATIONS
FOR A COMPRESSIBLE BOUNDARY LAYER
WITH WALL COOLING**

*JOHN E. YATES
COLEMAN duP. DONALDSON*

Approved for public release; distribution unlimited.

ie

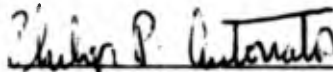
FOREWORD

This report was prepared by Aeronautical Research Associates of Princeton, Inc., Princeton, New Jersey, under Contract Number F33615-72-C-1350, Project No. 1366. The principal investigator was Dr. Coleman duP. Donaldson. The research covers the period from January 3, 1972 through October 4, 1972. The contractor's report number is A.R.A.P. Report No. 183.

This work was administered by the Air Force Flight Dynamics Laboratory, Air Force Systems Command, Wright-Patterson AFB, Ohio; the project monitor was Mr. E. D. McElderry (FXG).

The authors wish to thank Mr. Barry Gilligan for assistance with the computer programming and calculations; Mrs. Patricia Tobin for preparing the figures; and Mrs. Lois Ridgway for typing the report.

This technical report has been reviewed and is approved.



Philip P. Antonatos
Chief, Flight Mechanics Division
Air Force Flight Dynamics Laboratory

TABLE OF CONTENTS

SECTION	PAGE
I. INTRODUCTION.....	1
II. BASIC MODEL EQUATIONS AND METHOD OF SOLUTION	2
1. Model Equations.....	2
2. Definition of Transition.....	3
3. Initial Disturbance.....	4
III. DISCUSSION OF RUN-OUT CALCULATIONS.....	6
IV. CONCLUSIONS.....	9
V. RECOMMENDATIONS.....	10
REFERENCES.....	11
FIGURES.....	13

LIST OF ILLUSTRATIONS

- Figure 1a. Turbulent friction ratio Γ versus Reynolds number R_x ; wall temperature ratio $G_w = 0.05$.
- Figure 1b. Turbulent friction ratio Γ versus Reynolds number R_x ; wall temperature ratio $G_w = 0.2$.
- Figure 1c. Turbulent friction ratio Γ versus Reynolds number R_x ; wall temperature ratio $G_w = 0.5$.
- Figure 1d. Turbulent friction ratio Γ versus Reynolds number R_x ; wall temperature ratio $G_w = 0.75$.
- Figure 1e. Turbulent friction ratio Γ versus Reynolds number R_x ; wall temperature ratio $G_w = 1.0$.
- Figure 1f. Turbulent friction ratio Γ versus Reynolds number R_x ; wall temperature ratio $G_w = 1.2$.
- Figure 2. Transition and minimum critical R_x versus wall temperature ratio G_w .
- Figure 3. Comparison of minimum critical R_x in the frozen and growing mode.
- Figure 4. Comparison of R_x transition with experiment.
- Figure 5. Effect of initial disturbance level on R_{xtr} versus G_w at $M = 3$.
- Figure 6. Effect of initial disturbance level on transition and minimum critical (growing mode) at $M = 3$ and $G_w = 0.5$.
- Figure 7. Mean velocity, temperature and turbulent energy profiles for $M = 3$ and $G_w = 0.2$.
- Figure 8. Mean velocity, temperature and turbulent energy profiles for $M = 6$ and $G_w = 0.2$.
- Figure 9. Mean velocity, temperature and turbulent energy profiles for $M = 12$ and $G_w = 0.2$.
- Figure 10. Mean velocity, temperature and turbulent energy profiles for $M = 3$ and $G_w = 0.5$.
- Figure 11. Mean velocity, temperature and turbulent energy profiles for $M = 6$ and $G_w = 0.5$.

- Figure 12. Mean velocity, temperature and turbulent energy profiles for $M = 12$ and $G_w = 0.5$.
- Figure 13. Mean velocity, temperature and turbulent energy profiles for $M = 3$ and $G_w = 1.0$.
- Figure 14. Mean velocity, temperature and turbulent energy profiles for $M = 6$ and $G_w = 1.0$.
- Figure 15. Mean velocity, temperature and turbulent energy profiles for $M = 12$ and $G_w = 1.0$.

LIST OF SYMBOLS

a, b	dimensionless parameters in model equations
$C_{f_{turb}}$	$- 2\rho \overline{u'v'}$ turbulent friction coefficient
$C_{f_{wall}}$	$2 \frac{\mu_w}{R} \frac{\partial u}{\partial y} \Big _w$ wall friction coefficient
G_w	T_w/T_e^0 wall temperature ratio
h	spread of initial disturbance profile (see Eq. (2.12))
IK	total turbulent energy (see Eq. (2.13))
k_1, k_2, k_3	turbulent energy components
K	$k_1 + k_2 + k_3$
M	freestream Mach number
R	Reynolds number based on freestream velocity and viscosity and $\delta_{.99}$ at point of initial disturbance
R_x	Reynolds number based on wetted length along the flat plate
T	dimensionless temperature
T_e^0	freestream stagnation temperature
u, v	dimensionless mean velocity parallel and normal to the wall
u', v', w'	dimensionless perturbation velocity components
x, y	Cartesian coordinate system
y_c	point of maximum initial disturbance (see Eq. (2.12))
y_{sp}	integral spread of initial turbulence (see Eq. (2.13))
γ	ratio of specific heats
Γ	$C_{f_{turb}}/C_{f_{wall}}$

$\delta_{.99}$	boundary layer thickness where $u = 0.99$
λ	microscale of turbulence
μ	viscosity
ρ	dimensionless density
σ	$-\overline{u'v'}$

Subscripts

e	freestream condition
w	wall condition
(\bar{q})	average of quantity q

SECTION I

INTRODUCTION

In Reference 1 a model for studying the start of transition in a compressible boundary layer is developed. Extensive calculations are made over a wide range of Mach numbers and wall temperature ratios. Emphasis is placed on the development of the model equations and the calculation of minimum critical Reynolds number in a laminar compressible boundary layer. The present report is a natural sequel to Reference 1 in that the calculations are extended to the point where transition actually begins. Before we discuss the results of our present transition run-out calculations, we review a few of the key results of our previous study.

The main results in Reference 1 are based on linear equations for the turbulent energy components and velocity correlation. Following the approach of linear stability analysis, a mean parallel laminar flow is assumed. A small disturbance is inserted into the boundary layer at various Reynolds numbers and tracked downstream. The Reynolds number for which the initial disturbance neither grows nor decays downstream is defined to be "minimum critical." The rate at which disturbances grow or decay is related to the amplification rate calculated in classical stability analyses.

The principal conclusions of Reference 1 are the following:

1. Amplification rates agree in magnitude with those of classical stability calculation.
2. Increasing Mach number has a strong favorable effect on wetted length minimum critical Reynolds number.
3. Wall cooling has a favorable effect on minimum critical Reynolds number.
4. It is unwise to directly relate a minimum critical Reynolds number calculation to the prediction of transition Reynolds number.

Preliminary transition run-out calculations in Reference 1 suggest that increasing Mach number has a strong favorable effect on transition Reynolds number and that wall cooling has a favorable effect. In the present report a comprehensive set of transition run-out calculations over a wide range of Mach numbers and wall temperature rates is made. The results confirm and extend the preliminary findings of Reference 1. Comparisons with experimental results show conclusively that the analytic model is a useful tool for studying the start of compressible transition.

SECTION II

BASIC MODEL EQUATIONS AND METHOD OF SOLUTION

1. Model Equations

The basic equations to be used for our study of compressible transitions on a flat wall are derived in Reference 1. In dimensionless form they are:

$$\frac{\partial \rho u}{\partial x} + \frac{\partial \rho v}{\partial y} = 0 \quad (2.1)$$

$$\rho u \frac{\partial u}{\partial x} = -\rho v \frac{\partial u}{\partial y} + \frac{\partial}{\partial y} \left(\frac{\mu}{R} \frac{\partial u}{\partial y} + \rho \sigma \right) \quad (2.2)$$

$$\begin{aligned} \rho u \frac{\partial k_1}{\partial x} = & -\rho v \frac{\partial k_1}{\partial y} + 2\rho \sigma \frac{\partial u}{\partial y} + \frac{1}{R} \frac{\partial \mu}{\partial y} \frac{\partial}{\partial y} \left(2k_1 - \frac{K}{3} \right) \\ & + a\rho \frac{\partial u}{\partial y} \left(\frac{K}{3} - k_1 \right) + \frac{\mu}{R} \frac{\partial^2 k_1}{\partial y^2} - \frac{2\mu}{R} \frac{k_1}{\lambda^2} \end{aligned} \quad (2.3)$$

$$\begin{aligned} \rho u \frac{\partial k_2}{\partial x} = & -\rho v \frac{\partial k_2}{\partial y} + 2 \frac{\partial}{\partial y} \left(b\lambda^2 \rho \frac{\partial u}{\partial y} \frac{\partial k_2}{\partial y} \right) + \frac{1}{R} \frac{\partial \mu}{\partial y} \left(4k_2 - \frac{K}{3} \right) \\ & + a\rho \frac{\partial u}{\partial y} \left(\frac{K}{3} - k_2 \right) + \frac{\mu}{R} \frac{\partial^2 k_2}{\partial y^2} - \frac{2\mu}{R} \frac{k_2}{\lambda^2} \end{aligned} \quad (2.4)$$

$$\begin{aligned} \rho u \frac{\partial k_3}{\partial x} = & -\rho v \frac{\partial k_3}{\partial y} + \frac{1}{R} \frac{\partial \mu}{\partial y} \frac{\partial}{\partial y} \left(2k_3 - \frac{K}{3} \right) + a\rho \frac{\partial u}{\partial y} \left(\frac{K}{3} - k_3 \right) \\ & + \frac{\mu}{R} \frac{\partial^2 k_3}{\partial y^2} - \frac{2\mu}{R} \frac{k_3}{\lambda^2} \end{aligned} \quad (2.5)$$

$$\begin{aligned} \rho u \frac{\partial \sigma}{\partial x} = & -\rho v \frac{\partial \sigma}{\partial y} + \rho k_2 \frac{\partial u}{\partial y} + \frac{\partial}{\partial y} \left(b\lambda^2 \rho \frac{\partial u}{\partial y} \frac{\partial \sigma}{\partial y} \right) \\ & + \frac{3}{R} \frac{\partial \mu}{\partial y} \frac{\partial \sigma}{\partial y} - a\rho \frac{\partial u}{\partial y} \sigma + \frac{\mu}{R} \frac{\partial^2 \sigma}{\partial y^2} - \frac{2\mu}{R} \frac{\sigma}{\lambda^2} \end{aligned} \quad (2.6)$$

where

$$k_1 = \overline{u'u'} \quad , \quad k_2 = \overline{v'v'} \quad , \quad k_3 = \overline{w'w'}$$

$$K = k_1 + k_2 + k_3 \quad , \quad \sigma = -\overline{u'v'}$$

$$R = \frac{\rho_e u_e}{\mu_e} \delta_r$$

$$\mu = T^n$$

$$T = \left[G_w + (1 - G_w)u \right] \left(1 + \frac{\gamma - 1}{2} M^2 \right) - \frac{\gamma - 1}{2} M^2 u^2$$

$$G_w = \frac{T_w}{T_e} \quad (\text{dimensionless wall temperature}) \quad (2.7)$$

The integral length scale λ and the parameters a and b are the same as those used in Reference 1; namely,

$$\lambda = y$$

$$a = 5$$

$$b = 0$$

(2.8)

The reference length scale in all of the basic equations is the boundary layer thickness at the Reynolds number R . All velocities, thermodynamic variables and viscosity are scaled to their values at the edge of the boundary layer.

2. Definition of Transition

In our previous work, comprehensive calculations of minimum critical Reynolds number were made. There, Equations (2.3), (2.4), (2.5) and (2.6) were solved with a known mean velocity profile. The profile was not permitted to grow in the streamwise direction. The minimum critical Reynolds number was determined at which a given initial disturbance would neither grow nor decay downstream.

To determine the point at which transition actually begins, we proceed as follows. The equations for the turbulent energies and stress are coupled to the mean flow through Equation (2.2). We inject a disturbance into the boundary layer at some point upstream of the minimum critical point. The mean flow and

turbulence are then calculated simultaneously at points downstream to a point where the maximum turbulent stress grows to ten percent of the wall stress. The Reynolds number at this point is defined to be the "point of transition," ($R_{x_{tr}}$).

To make this definition precise we define a ratio of friction coefficients.

$$\Gamma = \frac{C_{f_{turb}}}{C_{f_{wall}}} \quad (2.9)$$

where (all quantities are dimensionless)

$$C_{f_{turb}} = -2\rho \overline{u'v'}$$

$$C_{f_{wall}} = 2 \frac{\mu_w}{R} \left. \frac{\partial u}{\partial y} \right|_w \quad (2.10)$$

The point of transition is the Reynolds number where

$$\Gamma = 0.1 \quad (2.11)$$

The actual transition Reynolds number $R_{x_{tr}}$ is based on the wetted length along the flat plate.

3. Initial Disturbance

In contrast to our previous study of minimum critical Reynolds number, the governing equations are now nonlinear. An obvious consequence is that the growth or decay of disturbances in the boundary layer is ultimately dependent on the magnitude and location of the initial disturbance. One of the main advantages of the present approach is that it provides a means for studying different kinds of initial disturbances. In the absence of any fundamental information on the generation of initial disturbances, e.g., by wall roughness, imposed sound field, or external turbulence, we have assumed the following standard input function. For each turbulent energy component we set

$$\frac{k}{k_{max}} = \left[1 - \left(\frac{y - y_c}{h} \right)^2 \right]^2 \quad (2.12)$$

where y_c is the location of the maximum energy and h is the spread. The total and maximum energy and integral spread are

given by

$$\begin{aligned} IK &= \int_0^{\delta} .99 K dy \\ k_{\max} &= \frac{IK}{3y_{sp}} \\ y_{sp} &= \frac{16}{15} h \end{aligned} \quad (2.13)$$

For all of the run-out calculations in this report we have set

$$y_c = y_{sp} = 0.5\delta \quad (2.14)$$

so that the initial turbulence is spread over the whole boundary layer with the maximum at one-half the thickness. For the majority of the calculations we have set

$$\begin{aligned} IK &= \int_0^{\delta} .99 K dy \\ &= 0.001 \end{aligned} \quad (2.15)$$

which is a measure of the turbulent energy density compared to the energy density of the mean flow at the edge of the boundary layer. Some results are presented to show the effect of various levels of disturbance on transition. Finally, we remark that the initial disturbance is injected at 0.8 of the minimum critical Reynolds number as determined in our previous study.

SECTION III

DISCUSSION OF RUN-OUT CALCULATIONS

Transition run-out calculations were made for Mach numbers $M = 0, 3, 6, 9, 12$ and wall temperature ratios ($G_w = T_w/T_e^0$) ranging from .05 to 1.2. The standard input disturbance with total turbulent energy level $IK = .001$ was used throughout the calculations except where noted otherwise.

In Figure 1, plates a to f, the results for the skin friction ratio ($\Gamma = C_{f_{turb}}/C_{f_{wall}}$) versus Reynolds number are presented for the range of parameters considered. Recall that the transition Reynolds number is the point where $\Gamma = 0.1$. For convenient reference, the minimum critical Reynolds number is also given for each run-out curve. For each wall temperature ratio, the increase in transition Reynolds number is apparent. An important feature of these curves is the very sharp increase in Γ with R_x at the point of transition, in particular at higher Mach numbers. This means that our basic definition of $R_{x_{tr}}$ is not too sensitive to the precise value chosen for Γ .

We note that each curve in Figure 1 has a minimum. The Reynolds number at or near this point* is the minimum critical Reynolds number for a growing boundary layer. These values are consistently larger than the minimum critical R_x for a frozen parallel flow. For higher Mach numbers the difference is appreciable. This suggests that the growth of the boundary layer has a strong stabilizing effect on small disturbances prior to transition that should be considered in the conventional linear stability analysis. Some recent studies of boundary layer stability have attempted to incorporate the growth effect although the results are inconclusive (see, e.g., Ref. 2). Finally, we remark that the minimum points in Figure 1 are not as sharply defined as the transition points.

The transition Reynolds numbers as deduced from Figure 1 are summarized in Figure 2 as a function of wall temperature for five Mach numbers. The minimum critical Reynolds numbers calculated in our previous work (Ref. 1) are also plotted for comparison. We note that $R_{x_{tr}}$ generally increases monotonically with Mach number or wall temperature ratio, although the Mach 12 curve has a minimum at very small G_w . The temperature effect is much less pronounced than the Mach number effect. A comparison of $R_{x_{tr}}$ with R_x minimum critical shows that wall cooling has exactly opposite effects, stabilizing transition and destabilizing minimum critical.

*Actually we have noted the point of minimum total energy which is the true definition of minimum critical.

The Mach number trend of $R_{x_{tr}}$ shown in Figure 2 is in agreement with experimental results (see discussion below). However, it is generally agreed experimentally (see Ref. 20, for example) that moderate wall cooling has a stabilizing effect on $R_{x_{tr}}$ while the opposite trend is indicated in Figure 2. The reason for the disagreement is believed to stem from our prescription of the initial disturbance. We have adopted a fixed value for the energy density IK (see (2.15)). The actual total disturbance energy is given by the product $\rho \cdot IK$. Since IK is fixed, a decrease in wall temperature (or increase in density) causes an increase in the total disturbance strength which in turn causes an earlier transition. A more detailed investigation of the actual strength of various initial disturbances and their dependence on wall cooling and Mach number will help to clarify this disparity.

In Figure 3 we compare R_x minimum critical calculated in the growing mode (dashed curves) with the frozen mode minimum critical results of our previous study (solid curves). The growing mode R_x generally increases with increasing wall temperature with a minimum and reverse trend at small values of G_w . The frozen mode R_x generally decreases with increasing wall temperature although the result for Mach 6 is an exception. We again note in Figure 3 that R_x growing mode is considerably larger than R_x frozen mode.

In Figure 4, $R_{x_{tr}}$ is plotted as a function of Mach number for three wall temperature ratios ($G_w = 0.2, 0.5, 1.0$). The results are compared with various experimental results reported in the literature (Refs. 3 through 17). Although the scatter in the experimental data precludes any detailed comparison, it is clear that the order of magnitude and general increasing trend of $R_{x_{tr}}$ with Mach number are in agreement between theory and experiment. The theory appears to increase somewhat more rapidly with Mach number than the experimental data.

In view of the uncertainties in existing experimental transition measurements and the somewhat arbitrary prescription of the theoretical initial disturbance, the overall agreement between theory and experiment is encouraging.

In Figures 5 and 6 some results are given to illustrate the effect of initial disturbance level on transition at $M = 3$. The disturbance level was first decreased to .0001 for various wall temperatures. The results in Figure 5 indicate that $R_{x_{tr}}$ is uniformly increased over the range of wall temperature ratios considered. In Figure 6 we plot R_x transition and R_x minimum critical, as computed in the growing mode, versus

initial disturbance level for $M = 3$ and $G_w = 0.5$. We note that $R_{x_{tr}}$ continually increases with decreasing disturbance level, whereas R_x minimum critical seems to approach an asymptotic value of approximately 2.36×10^5 . This limit value is higher than $R_{x_{tr}}$ minimum critical as computed in the frozen mode ($\approx 5 \times 10^4$).

In Figure 7 through 15, the mean velocity, temperature, and turbulent energy profiles are plotted for various Mach number and wall temperature combinations. For each value of M and G_w , we plot the profiles at R_x growing mode minimum critical and R_x transition. Because of the low turbulence levels, the mean velocity and temperature profiles are essentially self-similar over the entire Reynolds number range. Also, there is a very strong tendency towards isotropy in the present model, so that K is a measure of any one of the three energy components.

For fixed Mach number, the peak turbulent energy is shifted towards the wall and becomes more sharply concentrated as R_x tends to the point of transition. For larger values of the Mach number, the turbulent energy is more concentrated towards the outer edge of the boundary layer. For example, comparing Figures 13 and 15 at $G_w = 1.0$ and $R_{x_{tr}}$, the peak energy is at $y/\delta = 0.5$ for $M = 3$ and at $y/\delta = 0.75$ at $M = 12$. Recent experimental results (Ref. 18) on hypersonic transition show that the transition process actually starts at the outer edge of the boundary layer and is detected at the wall several boundary layer thicknesses downstream. This qualitative behavior is predicted by the present model.

SECTION IV
CONCLUSIONS

1. Increasing Mach number at constant wall temperature has a strong favorable effect on the transition Reynolds number. The Mach number trend of R_{xtr} is in general agreement with experimental results.
2. For fixed initial disturbance energy density, wall cooling at constant Mach number has an adverse effect on transition. Also, wall cooling generally has an adverse effect on the growing mode minimum critical R_x but favorable effect on the frozen mode minimum critical (see discussion, page 7).
3. The transition Reynolds number increases without bound as the level of the initial disturbance is decreased.
4. The minimum critical Reynolds number calculated for a growing boundary layer is larger than minimum critical for a parallel flow.
5. At hypersonic Mach numbers, the initial distribution of turbulent energy is concentrated near the outer edge of the boundary layer in agreement with experimental findings.
6. Based on comparisons with experimental results, we conclude that the analytical model is a useful guide for studying the start of transition in a compressible boundary layer.

SECTION V
RECOMMENDATIONS

Based on the successful stability calculations in Reference 1 and the transition run-out calculations presented here, it is recommended that:

1. The model be modified to treat the flow over a cone. Both stability and run-out calculations should be made.
2. The effects of external and wall disturbances be studied with the present model. These should include:
 - a. Wall roughness
 - b. External background turbulence
 - c. Externally imposed sound field.
3. The results of the present simplified model be used to supplement the further development of the full compressible model studied in Reference 19.

REFERENCES

1. Donaldson, C. duP., Sullivan, R.D. and Yates, J.E.: "An Attempt to Construct an Analytic Model of the Start of Compressible Transition," AFFDL TR-70-153, January 1971. Also see (U) Proceedings of the Boundary Layer Transition Workshop held 3-5 November 1971, Aerospace Report No. TOR-0172(S2816-16)-5, December 1971.
2. Boehman, L.I.: "Recalculation of Brown's Stability Results," (U) Proceedings of the Boundary Layer Transition Workshop held 3-5 November 1971, Aerospace Report No. TOR-0172 (S2816-16)-5, December 1971.
3. Maddalon, Dal V. and Henderson, Arthur: "Boundary-Layer Transition on Sharp Cones at Hypersonic Mach Numbers," AIAA Journal, Vol. 6, No. 4, March 1968, p. 424.
4. McCauley, W.D., Saydah, A.R. and Bueche, J.F.: "Effect of Spherical Roughness on Hypersonic Boundary-Layer Transition," AIAA Journal, Vol. 4, No. 12, December 1966, pp. 2142-2148.
5. Sanator, R.J., DeCarlo, J.P. and Torillo, D.T.: "Hypersonic Boundary-Layer Transition Data for a Cold-Wall Slender Cone," AIAA Journal, Vol. 3, No. 4, April 1965, pp. 758-760.
6. Stetson, K.F. and Rushton, G.H.: "A Shock Tunnel Investigation of the Effects of Nose Bluntness, Angle of Attack, and Boundary Layer Cooling on Boundary Layer Transition at a Mach Number of 5.15," AIAA Paper No. 66-495, Los Angeles, June 1966.
7. Stainback, C.P.: "Some Effects of Roughness and Variable Entropy on Transition at a Mach Number of 8," AIAA Paper No. 67-132, New York, January 1967. See also NASA TN D-4961, January 1969.
8. Softley, E.J., Graber, B.C. and Zempel, R.C.: "Experimental Observation of Transition of the Hypersonic Boundary Layer," AIAA Paper No. 68-39, 1968.
9. Softley, E.J.: "Transition of the Hypersonic Boundary Layer on a Cone. Part II, Experiments at $M = 10$ and More on Blunt-Cone Transition," GE Space Science Lab., MSD, Document No. GE-TIS-R68SD14, October 1968.
10. DiCristina, V.: "Three-Dimensional Laminar Boundary-Layer Transition on a Sharp 8° Cone at Mach 10," AIAA Journal, Vol. 8, No. 5, May 1970, p. 852.
11. Tani, I.: Boundary Layer Transition, Annual Reviews of Fluid Mechanics, Vol. I (Annual Reviews, Inc., Palo Alto, 1969).

12. Nagamatsu, H.T., Graber, B.C. and Sheer, R.E.: "Roughness, Bluntness, and Angle-of-Attack Effects on Hypersonic Boundary Layer Transition," J. Fluid Mech., Vol. 24, Part 1, January 1966, pp. 1-31.
13. Sheetz, N.W., Jr.: Boundary Layer Transition on Cones at Hypersonic Speeds, Proc. Navy-NASA-LTV Symposium on Viscous Drag Reduction (Plenum Press 1969).
14. Schubauer, G.G. and Skramstad, H.K.: "Laminar Boundary Layer Oscillations and Transition on a Flat Plate," NACA Report 909, 1948; J. Research National Bureau of Standards 38, 1947, pp. 251-292; J. Aero. Sci. 14, 1947, pp. 69-78.
15. Cary, A.M., Jr.: "Turbulent Boundary-Layer Heat Transfer and Transition Measurements for Cold Wall Conditions at Mach 6," AIAA Journal, Vol. 6, No. 5, May 1968, pp. 958-959.
16. Deem, R.E. and Murphy, J.S.: "Flat Plate Boundary Layer Transition at Hypersonic Speeds," AIAA Paper No. 65-128, January 1965.
17. Whitfield, J.D. and Iannuzzi, F.A.: "Experiments on Roughness Effects on Cone Boundary Layer Transition up to Mach 16," AIAA Journal, Vol. 7, No. 3, March 1969, pp. 465-470.
18. Beckwith, I.E. and Bertram, M.H.: "A Survey of NASA Langley Studies on High-Speed Transition and the Quiet Tunnel," NASA TM X-2566, July 1972.
19. Donaldson, C. duP. and Sullivan, R.D.: "An Invariant Second-Order Closure Model of the Compressible Turbulent Boundary Layer on a Flat Plate," A.R.A.P. Report No. 178, June 1972.
20. Morkovin, Mark V.: "Critical Evaluation of Transition from Laminar to Turbulent Shear Layers with Emphasis on Hypersonically Traveling Bodies," AFFDL-TR-68-149, March 1969.

$G_w = 0.05$

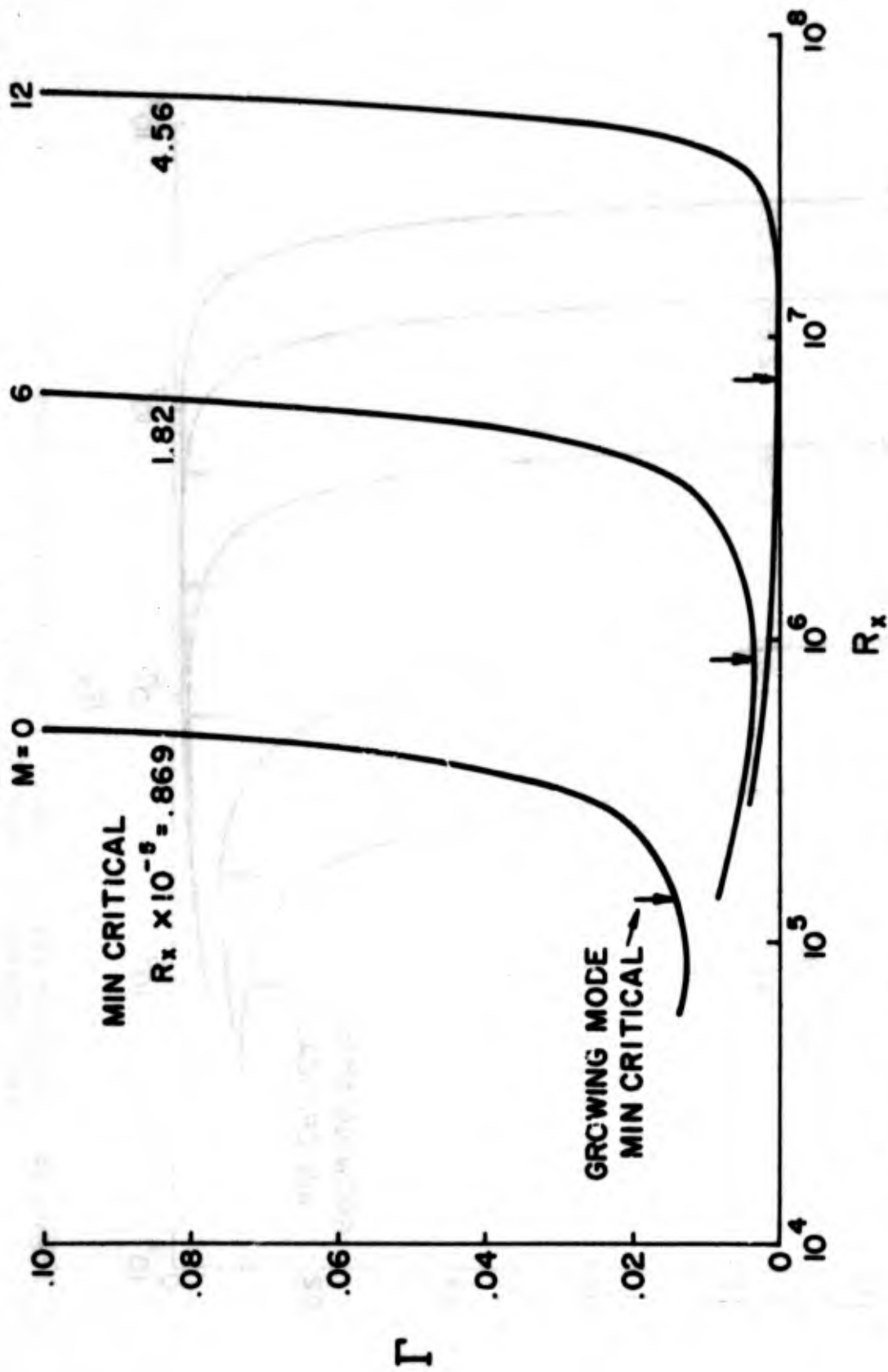


Figure 1a. Turbulent friction ratio Γ versus Reynolds number R_x ; wall temperature ratio $G_w = 0.05$.

$G_w = 0.2$

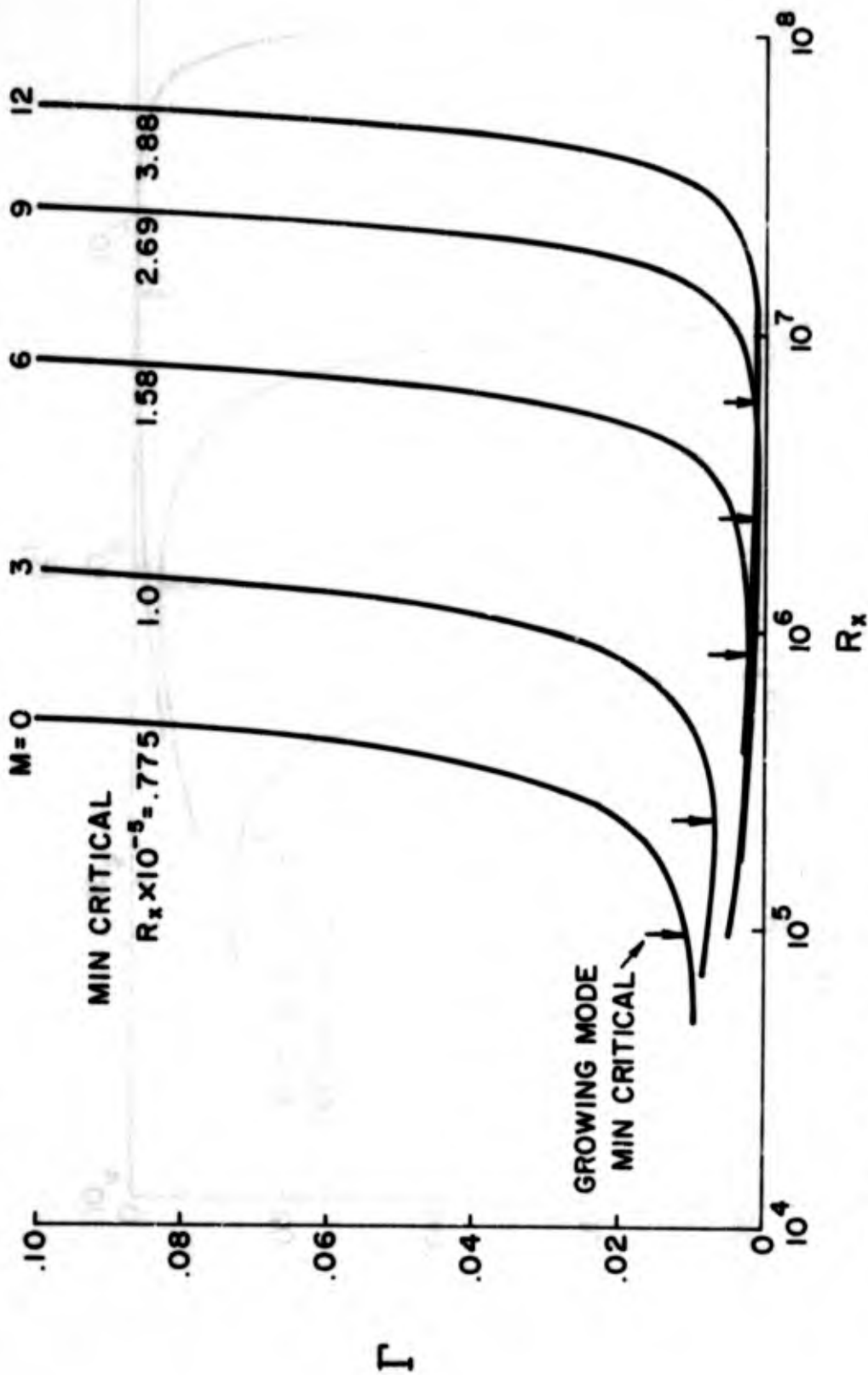


Figure 1b. Turbulent friction ratio Γ versus Reynolds number R_x ; wall temperature ratio $G_w = 0.2$.

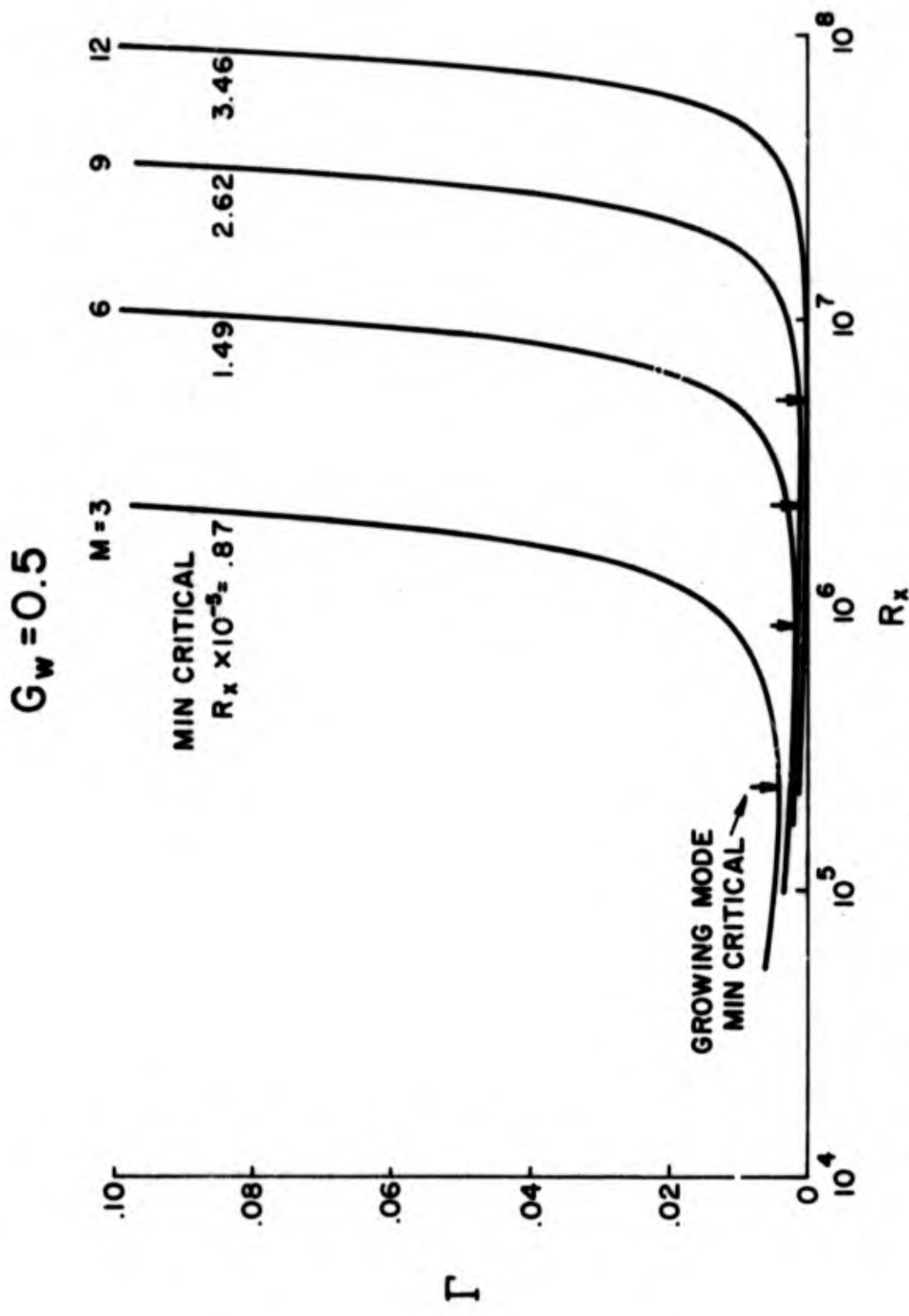


Figure 1c. Turbulent friction ratio Γ versus Reynolds number R_x ;
 wall temperature ratio $G_w = 0.5$.

$G_w = 0.75$

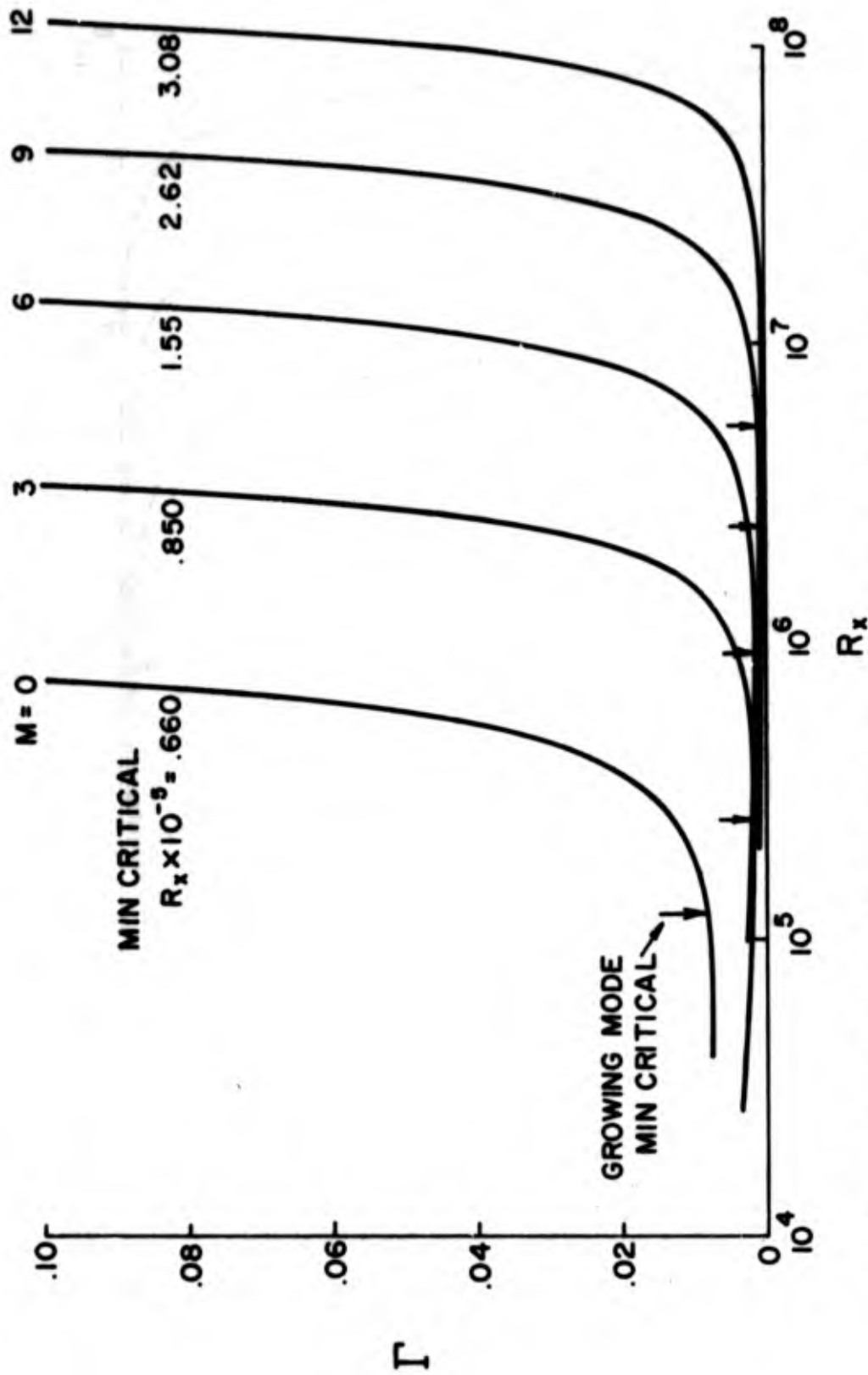


Figure 1d. Turbulent friction ratio Γ versus Reynolds number R_x ; wall temperature ratio $G_w = 0.75$.

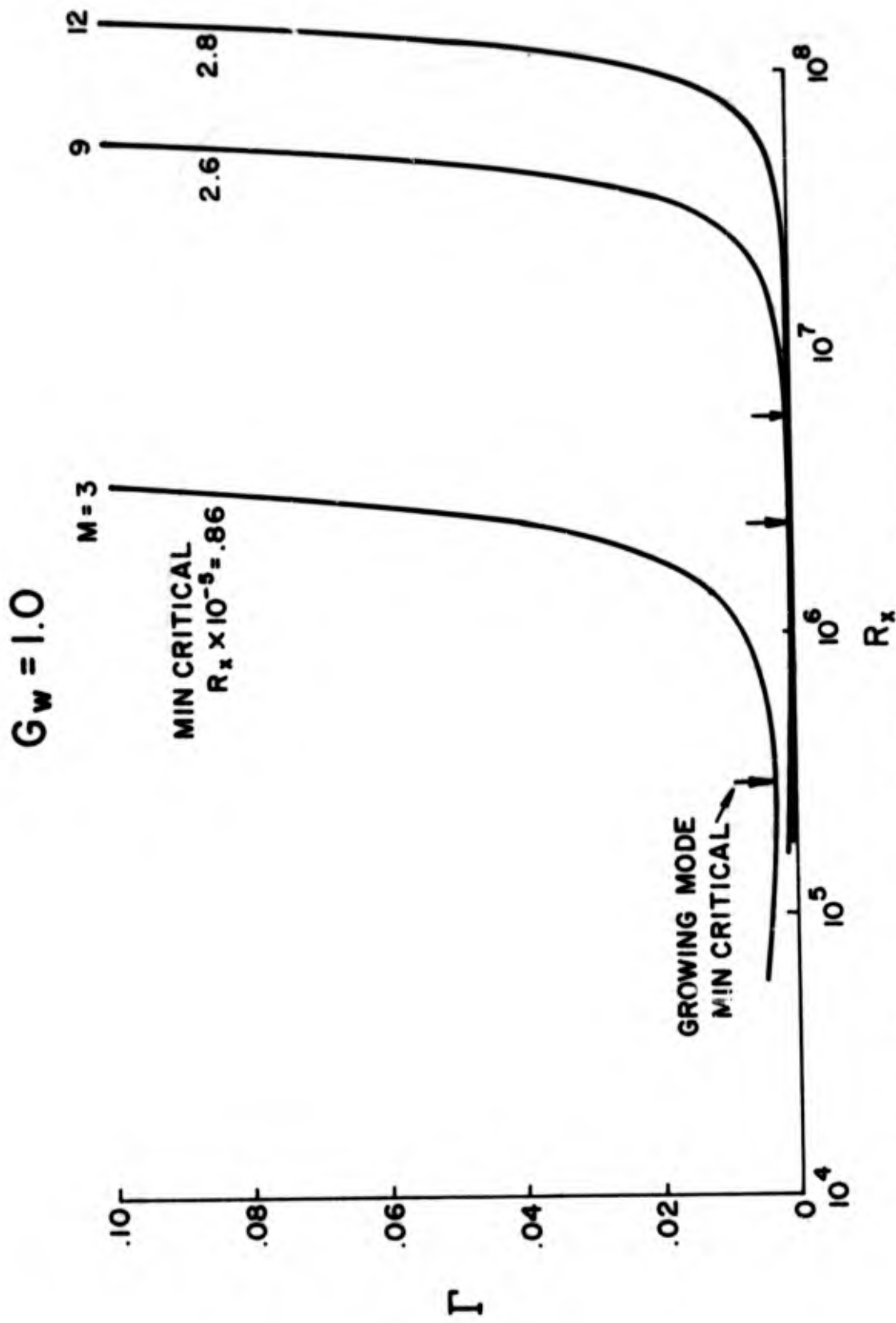


Figure 1e. Turbulent friction ratio Γ versus Reynolds number R_x ; wall temperature ratio $G_w = 1.0$.

$G_w = 1.2$

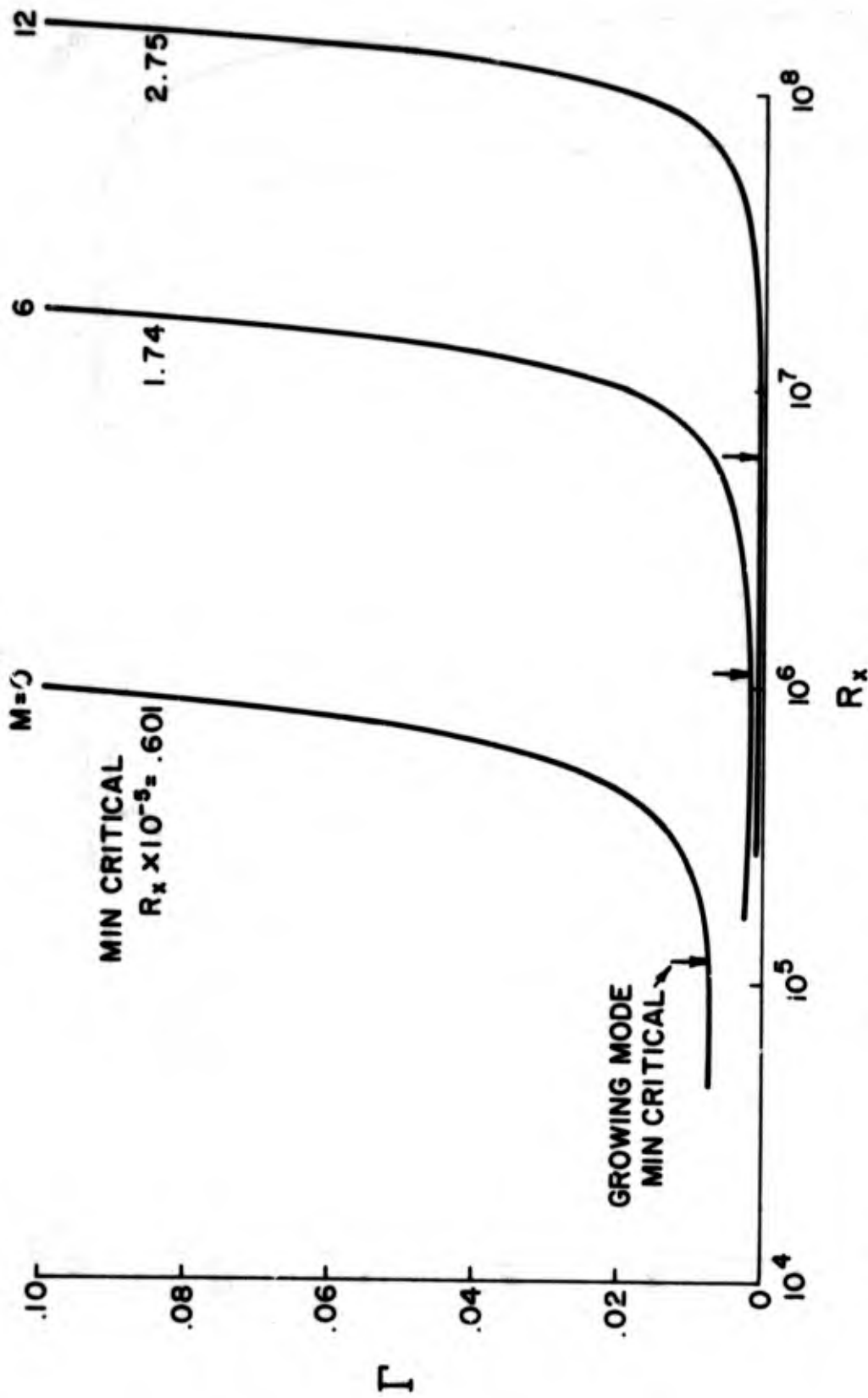


Figure 1f. Turbulent friction ratio Γ versus Reynolds number R_x ; wall temperature ratio $G_w = 1.2$.

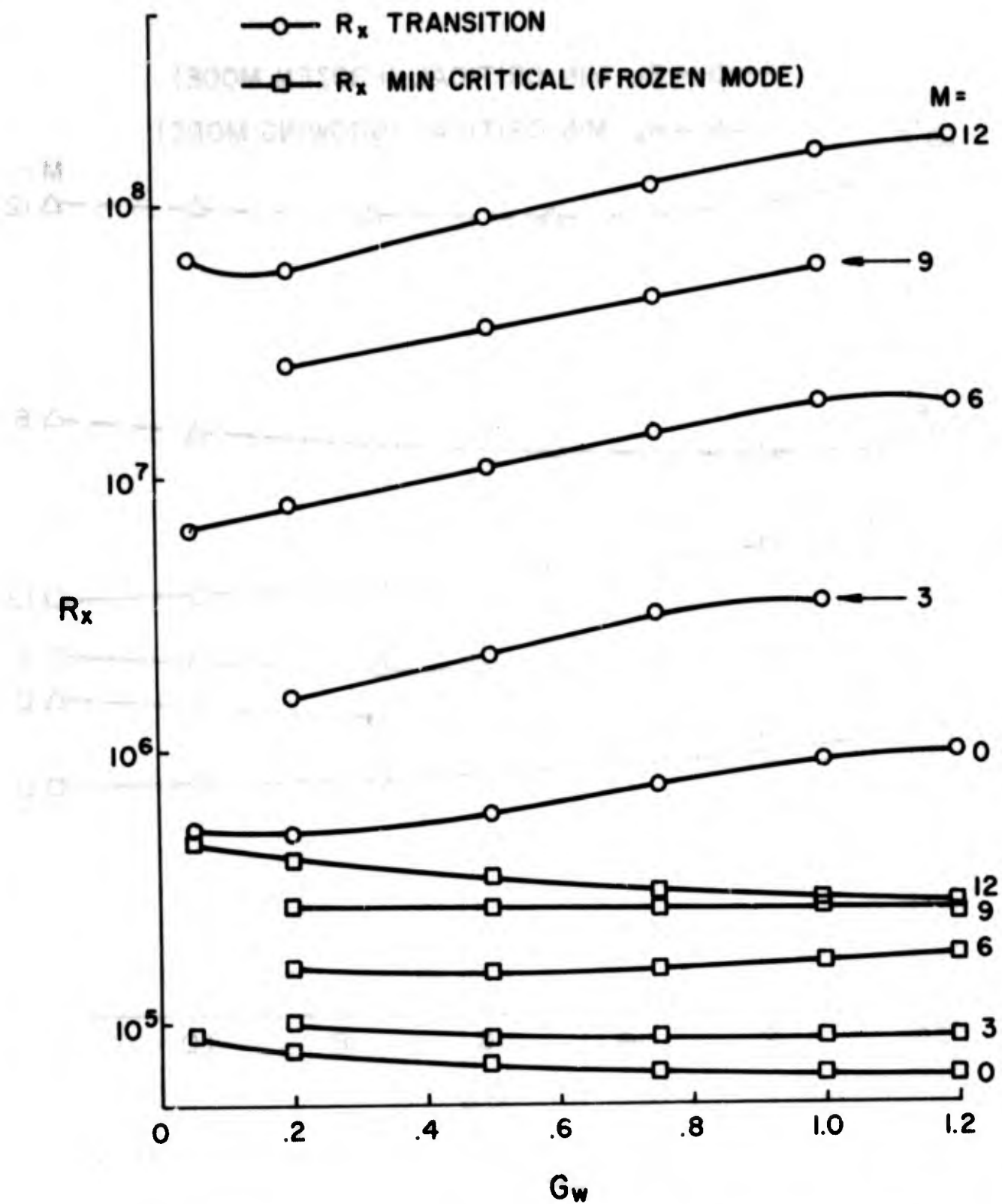


Figure 2. Transition and minimum critical R_x versus wall temperature ratio G_w .

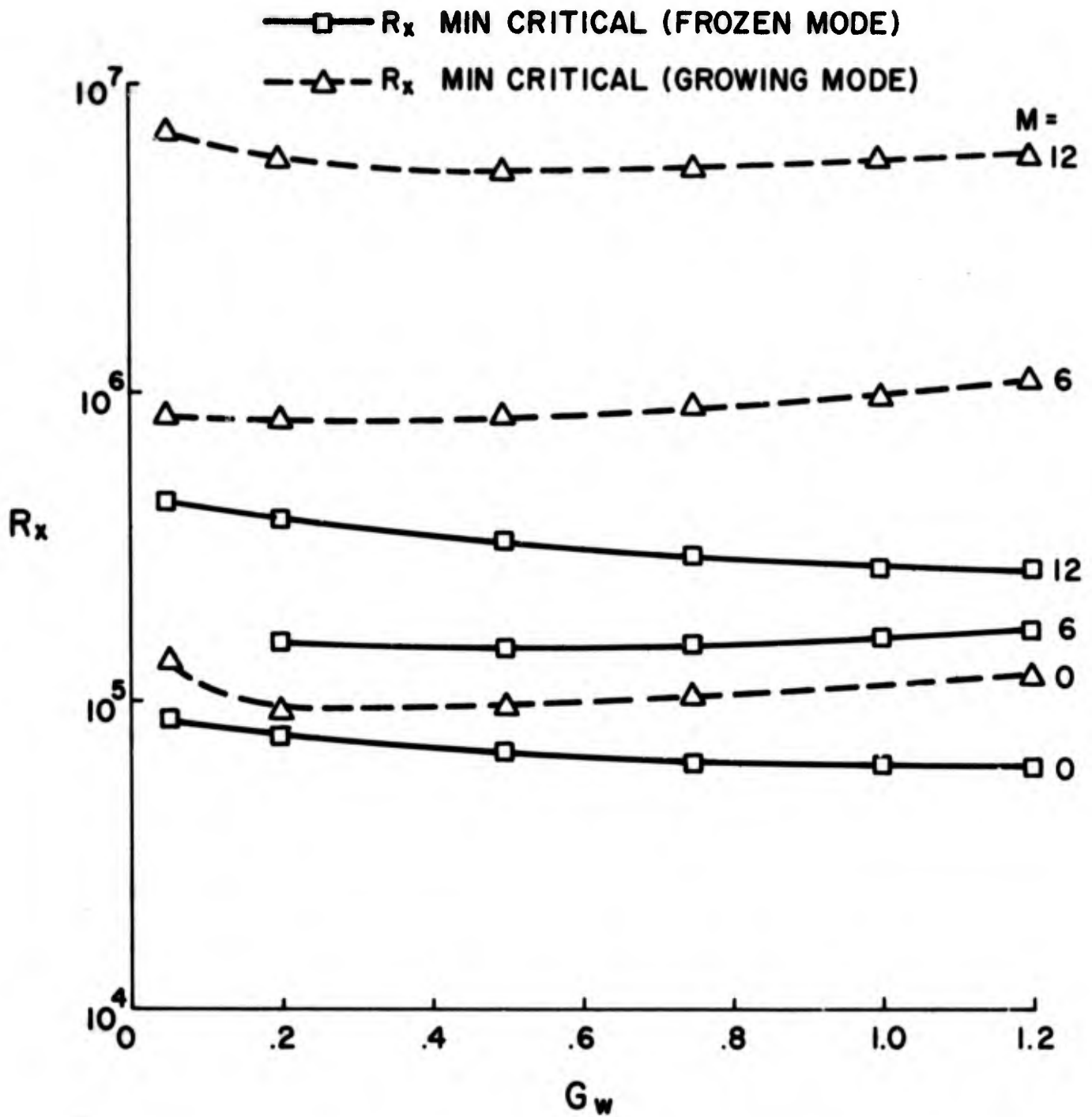


Figure 3. Comparison of minimum critical R_x in the frozen and growing mode.

- | | |
|-----------------------------|----------------------------|
| ○ MADDALON, HENDERSON | I SHEETZ |
| ▽ MCCAULEY, SAYDAH, BUECHE | ▷ SCHUBAUER, SKRAMSTAD |
| △ SANATOR, DECARLO, TORILLO | ♣ CARY |
| ◇ STETSON, RUSHTON | ∇ DEIM, MURPHY |
| ○ STAINBACK | △ WHITFIELD, IANUZZI |
| ◊ MATEER, LARSON | × DI CRISTINA |
| □ SOFTLEY, GRABER, ZEMPEL | ○ TANI |
| ◻ SOFTLEY | ▲ NAGAMATSU, GRABER, SHEER |
| — PRESENT THEORY | |

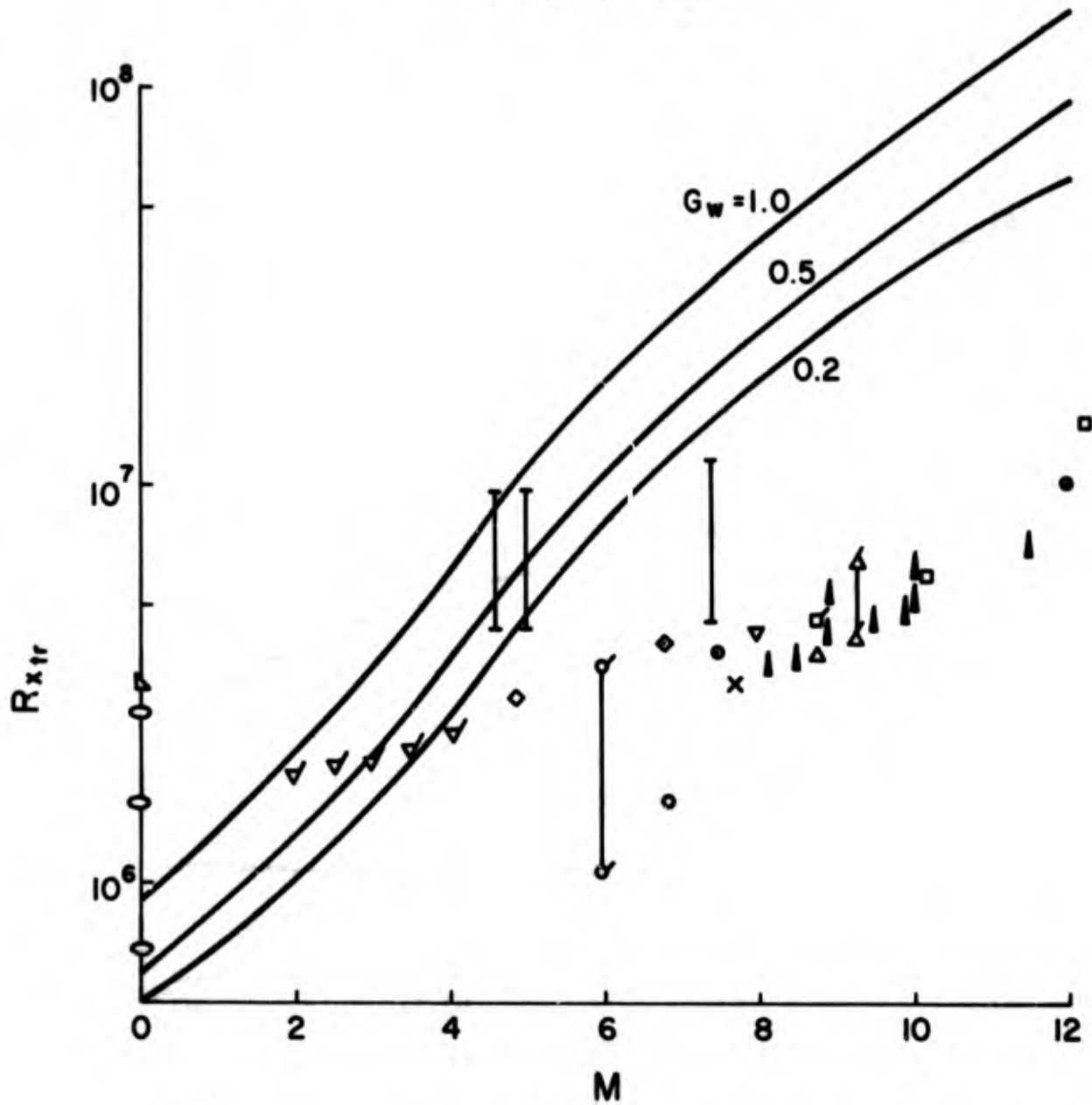


Figure 4. Comparison of $R_{x,tr}$ transition with experiment.

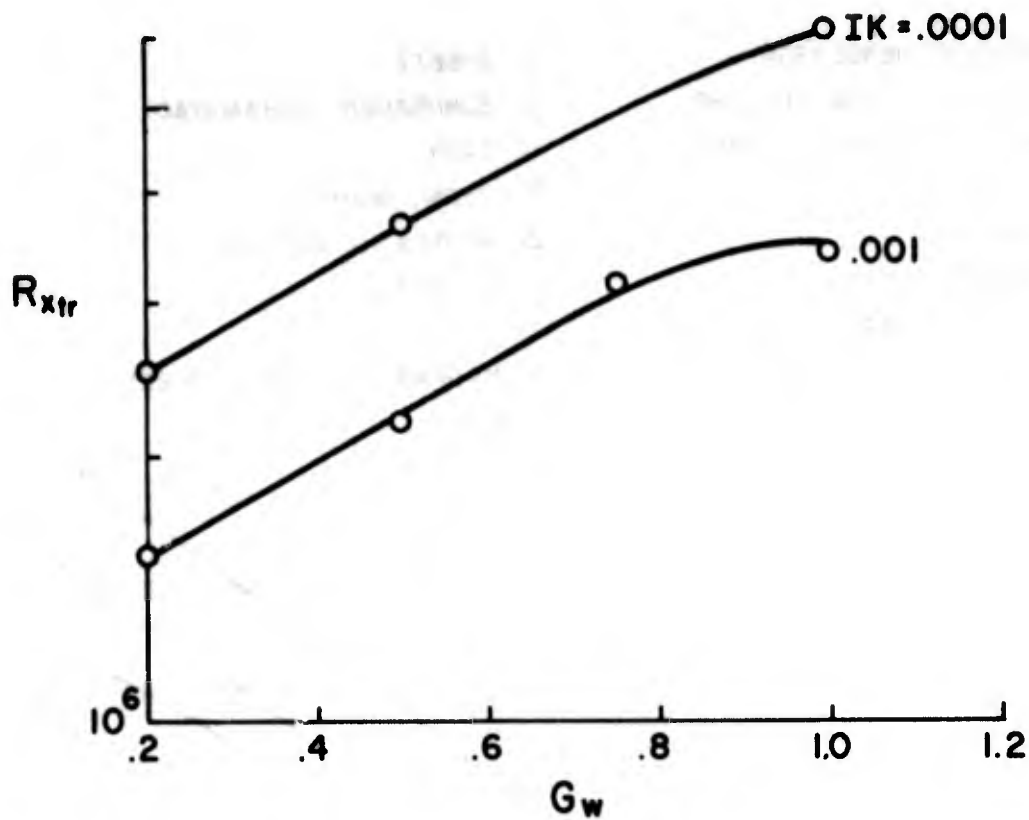


Figure 5. Effect of initial disturbance level on $R_{x_{tr}}$ versus G_w at $M = 3$.

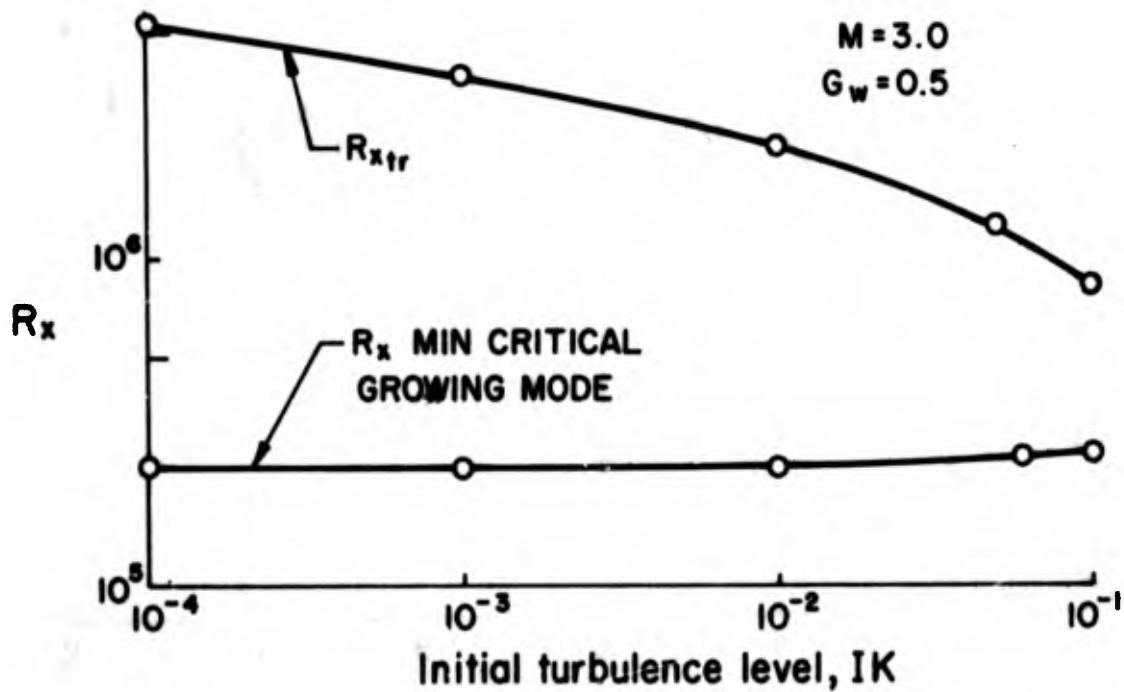


Figure 6. Effect of initial disturbance level on transition and minimum critical (growing mode) at $M = 3$ and $G_w = 0.5$.

$M = 3.0$
 $G_w = 0.2$

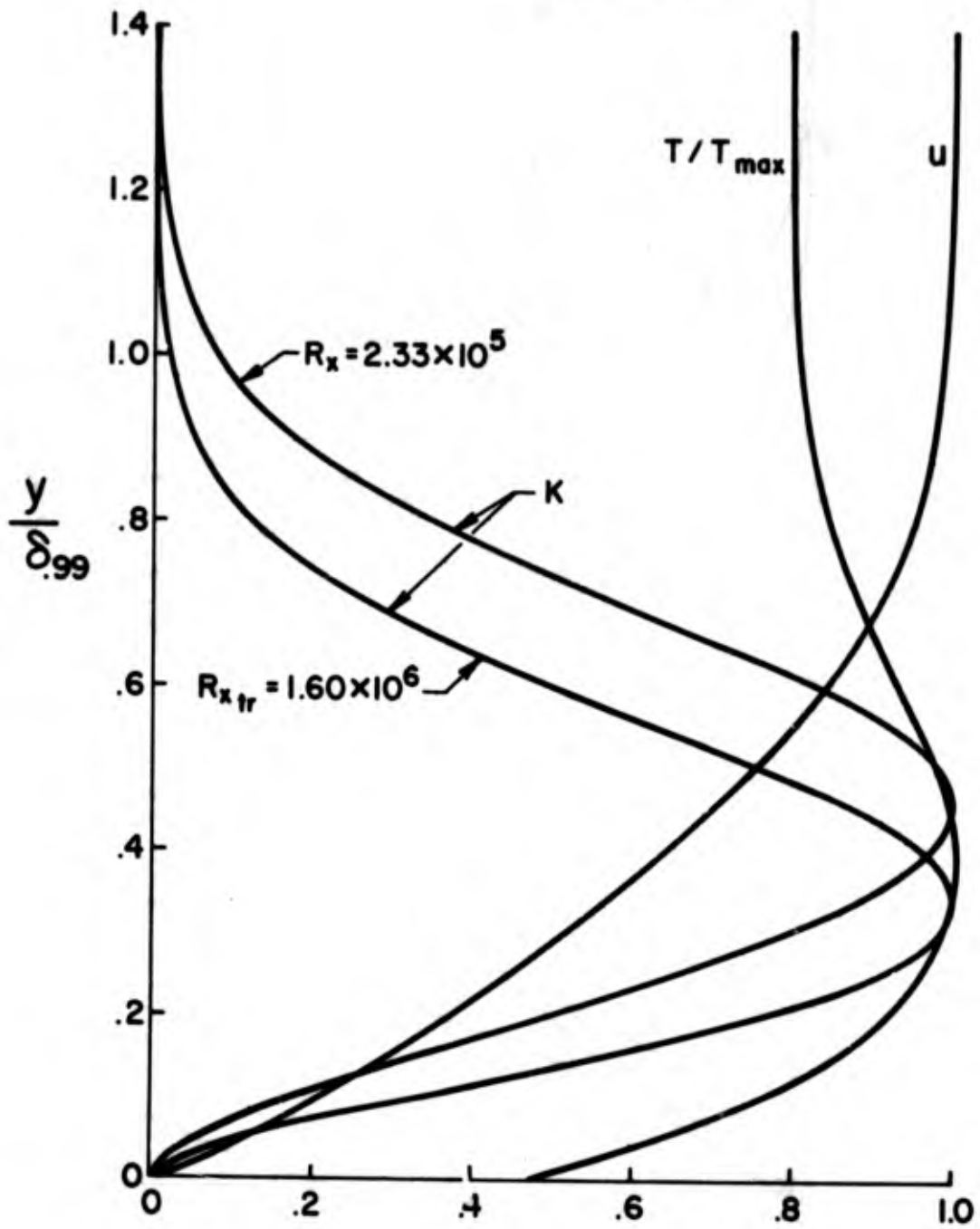


Figure 7. Mean velocity, temperature and turbulent energy profiles for $M = 3$ and $G_w = 0.2$.

M=6.0
G_w=0.2

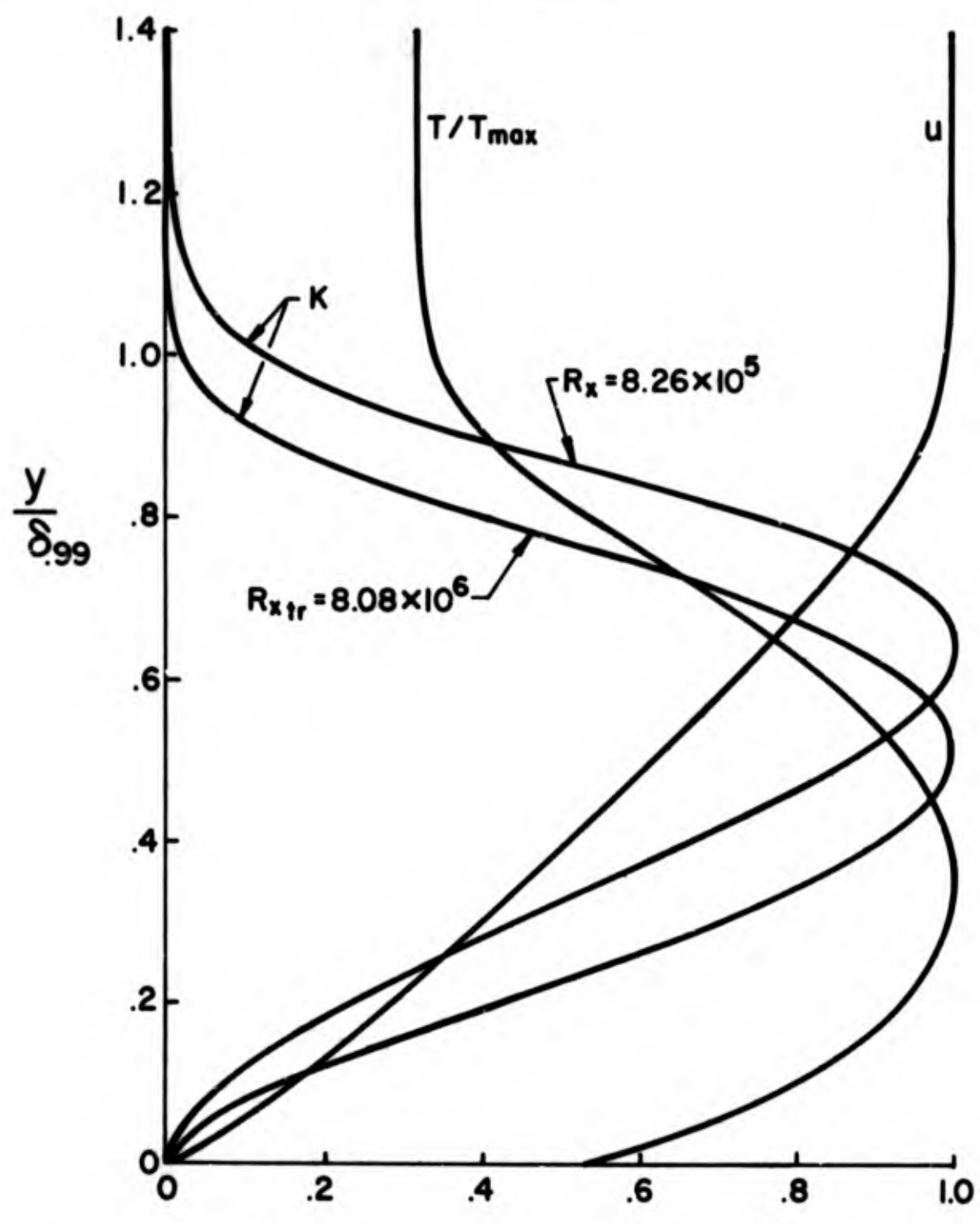


Figure 8. Mean velocity, temperature and turbulent energy profiles for $M = 6$ and $G_w = 0.2$.

$M=12.0$
 $G_w=0.2$

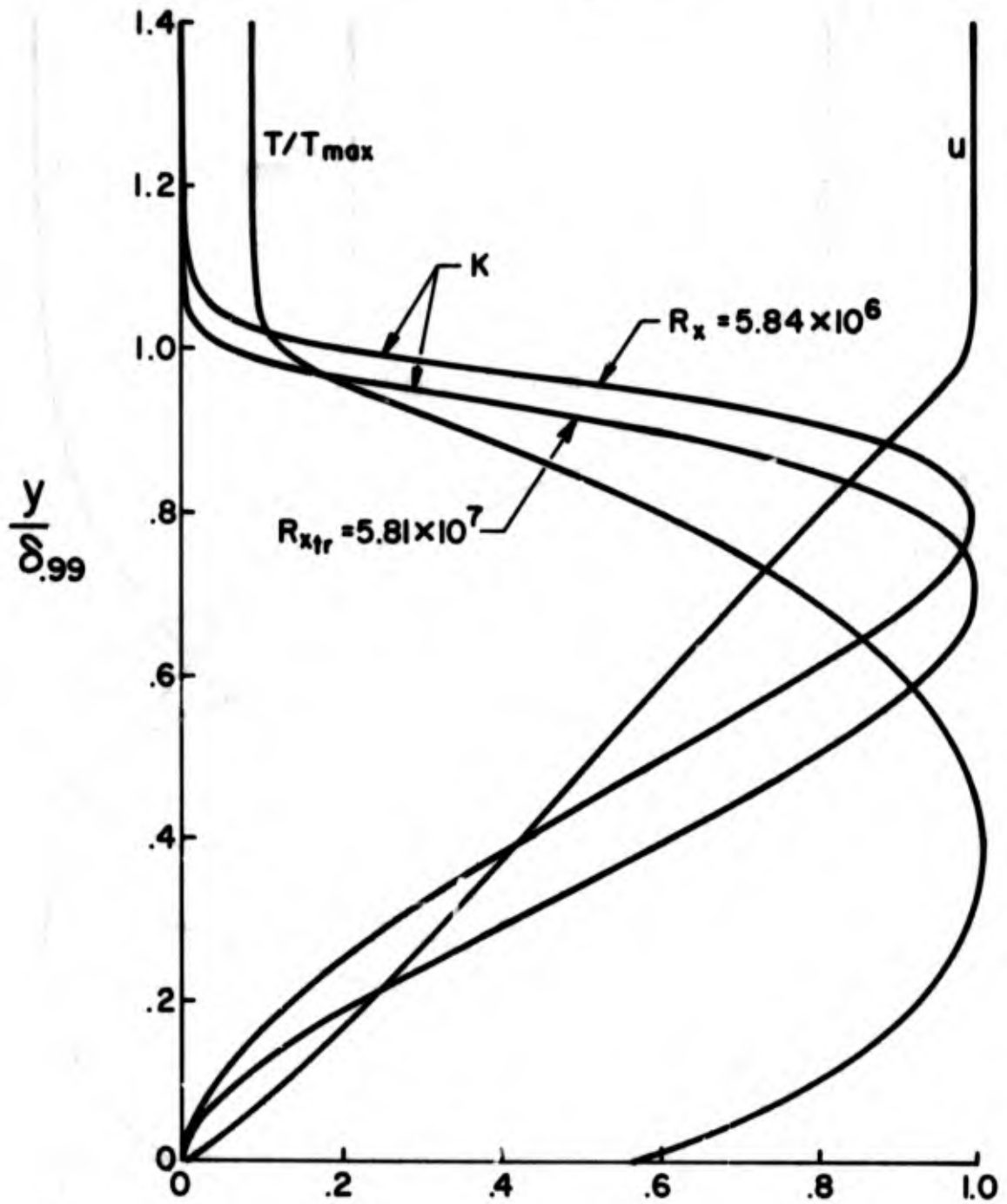


Figure 9. Mean velocity, temperature and turbulent energy profiles for $M = 12$ and $G_w = 0.2$.

$M=3.0$
 $G_w=0.5$

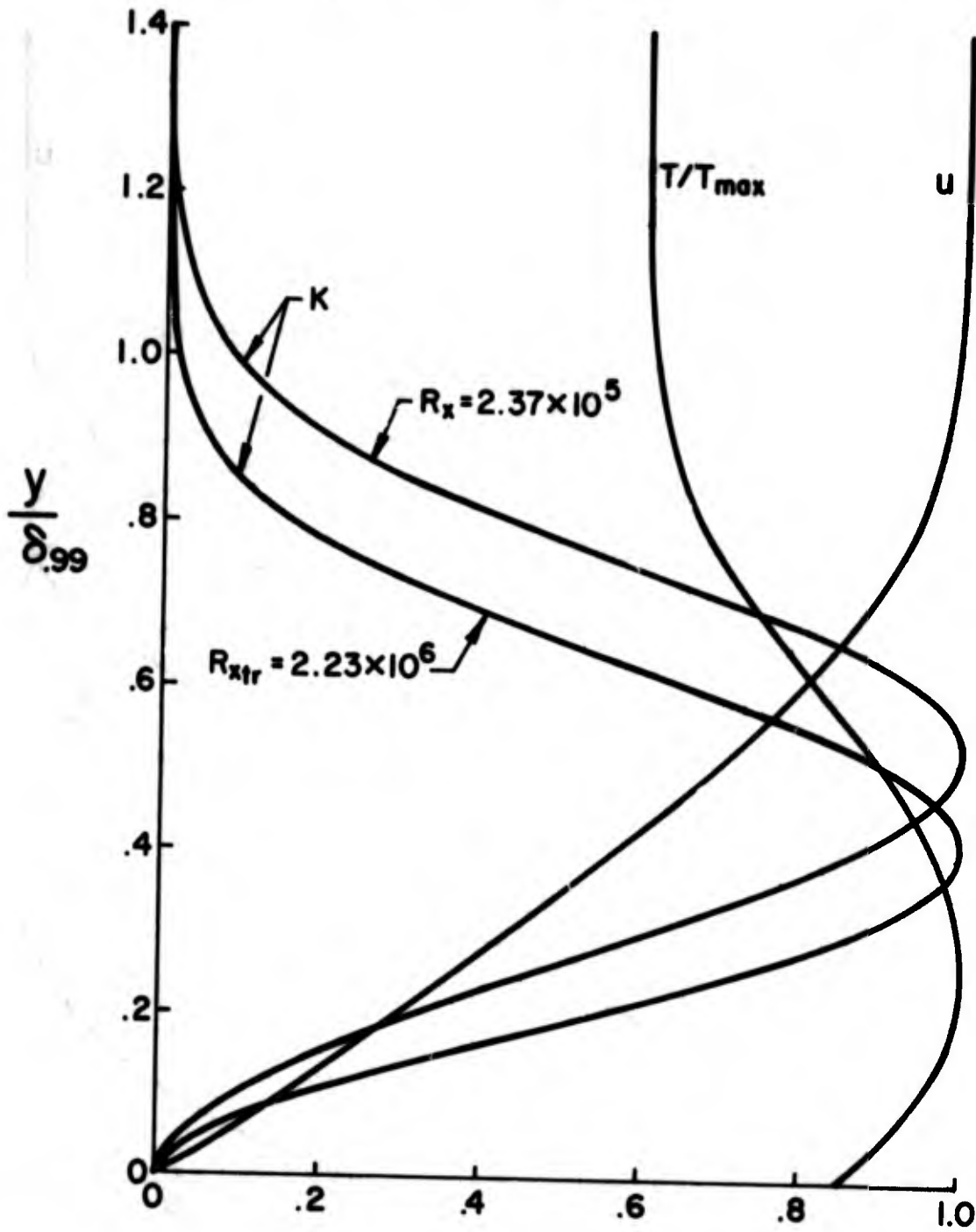


Figure 10. Mean velocity, temperature and turbulent energy profiles for $M = 3$ and $G_w = 0.5$.

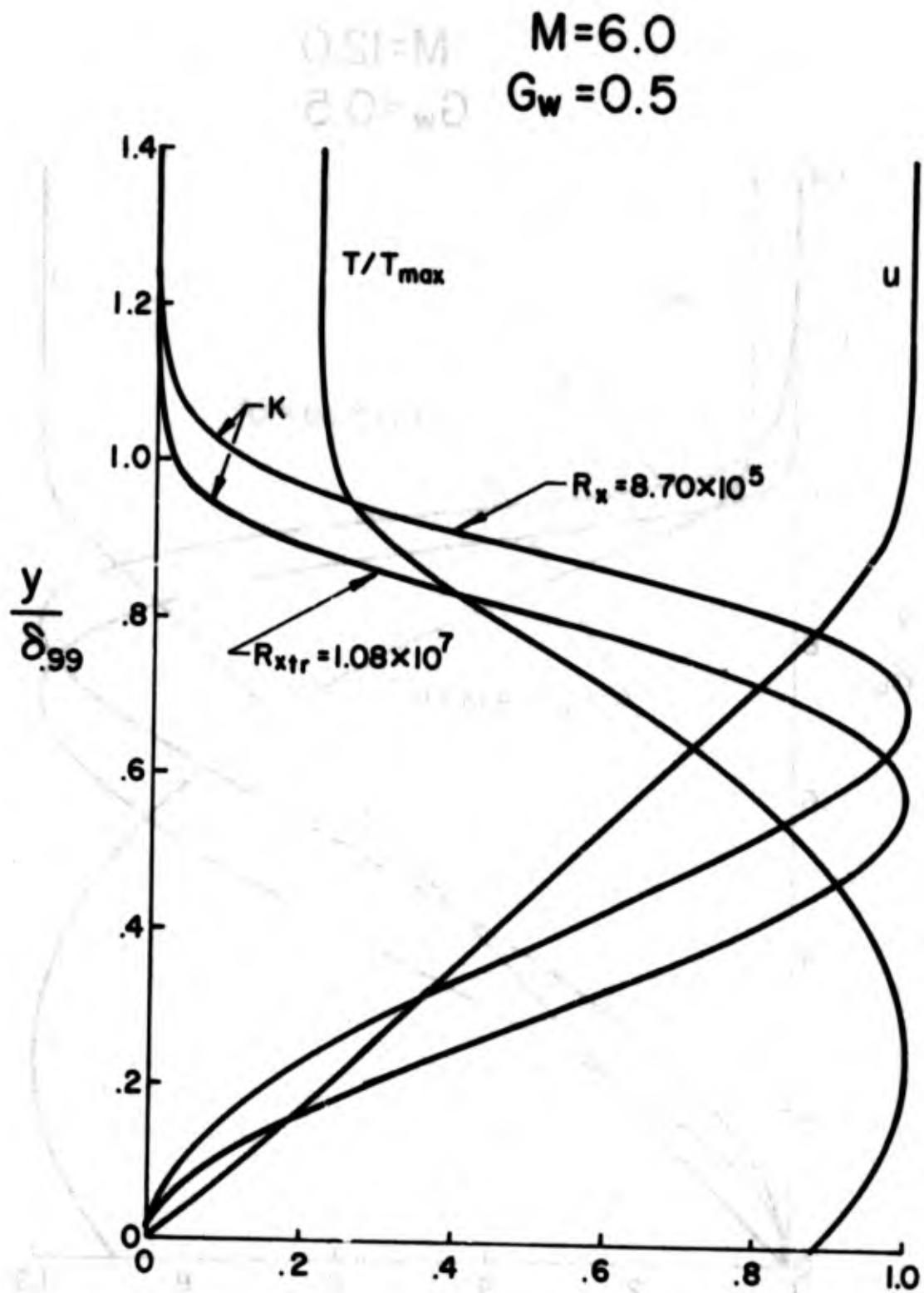


Figure 11. Mean velocity, temperature and turbulent energy profiles for $M = 6$ and $G_w = 0.5$.

$M=12.0$
 $G_w=0.5$

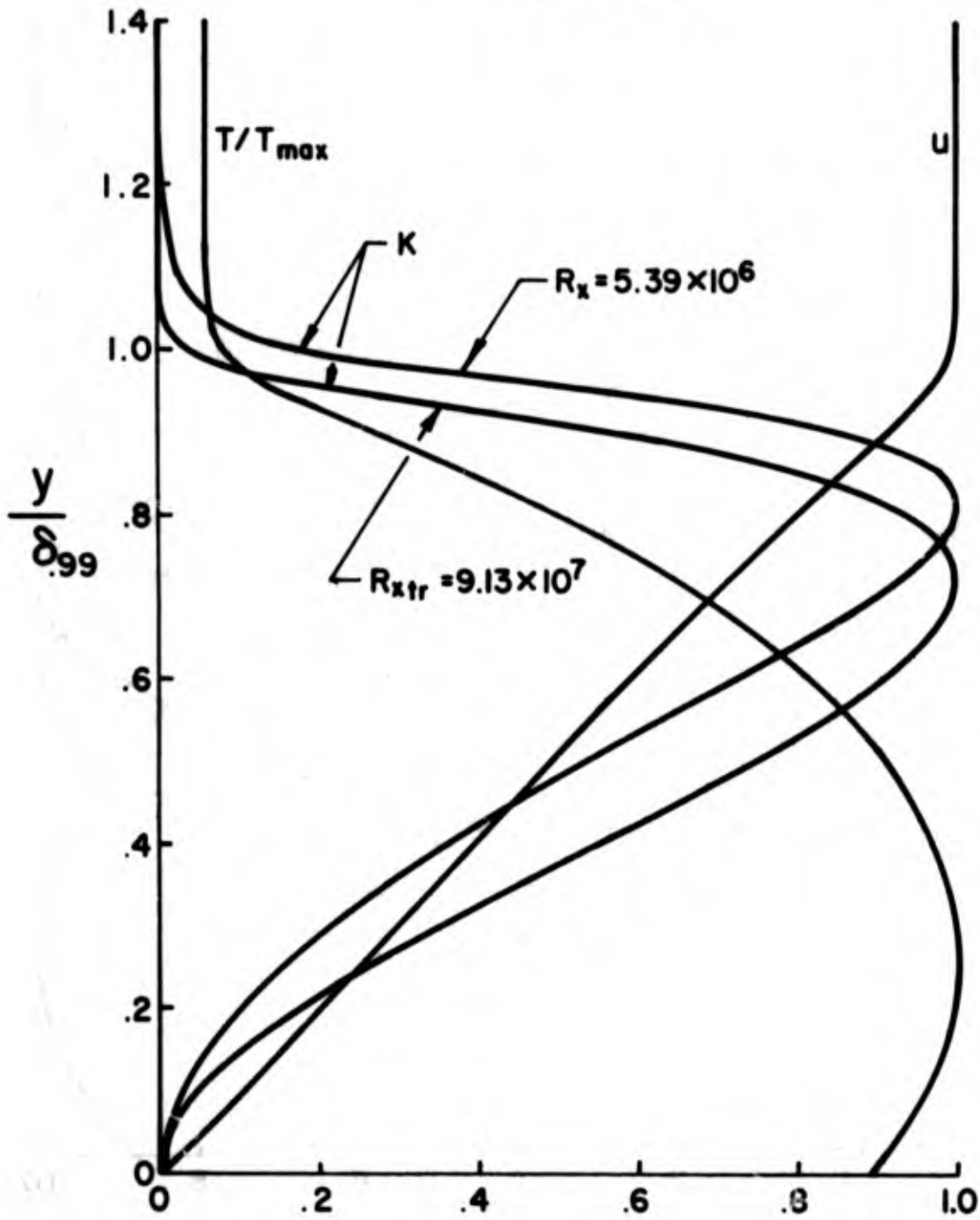


Figure 12. Mean velocity, temperature and turbulent energy profiles for $M = 12$ and $G_w = 0.5$.

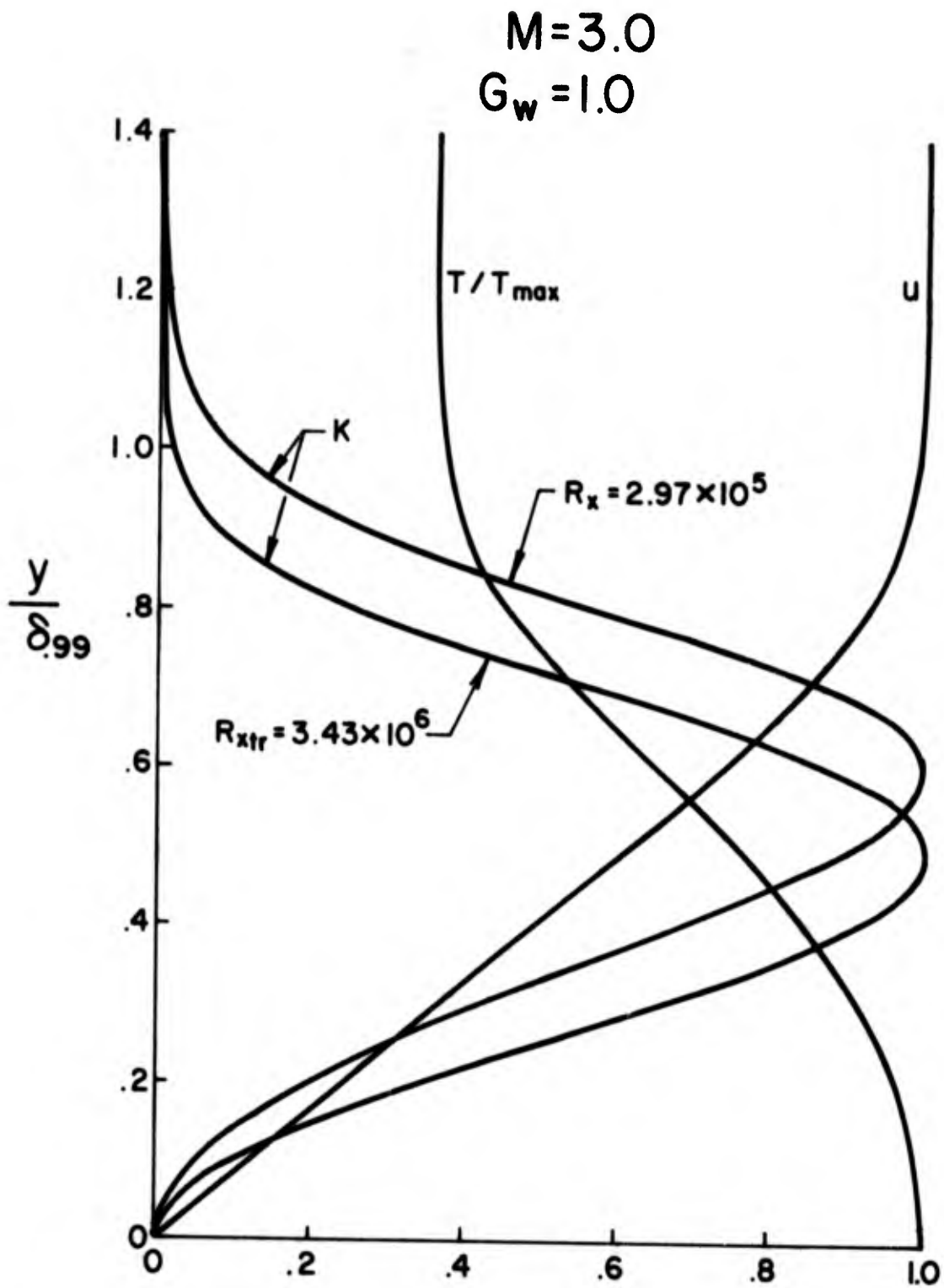


Figure 13. Mean velocity, temperature and turbulent energy profiles for $M = 3$ and $G_w = 1.0$.

M=6.0
G_w=1.0

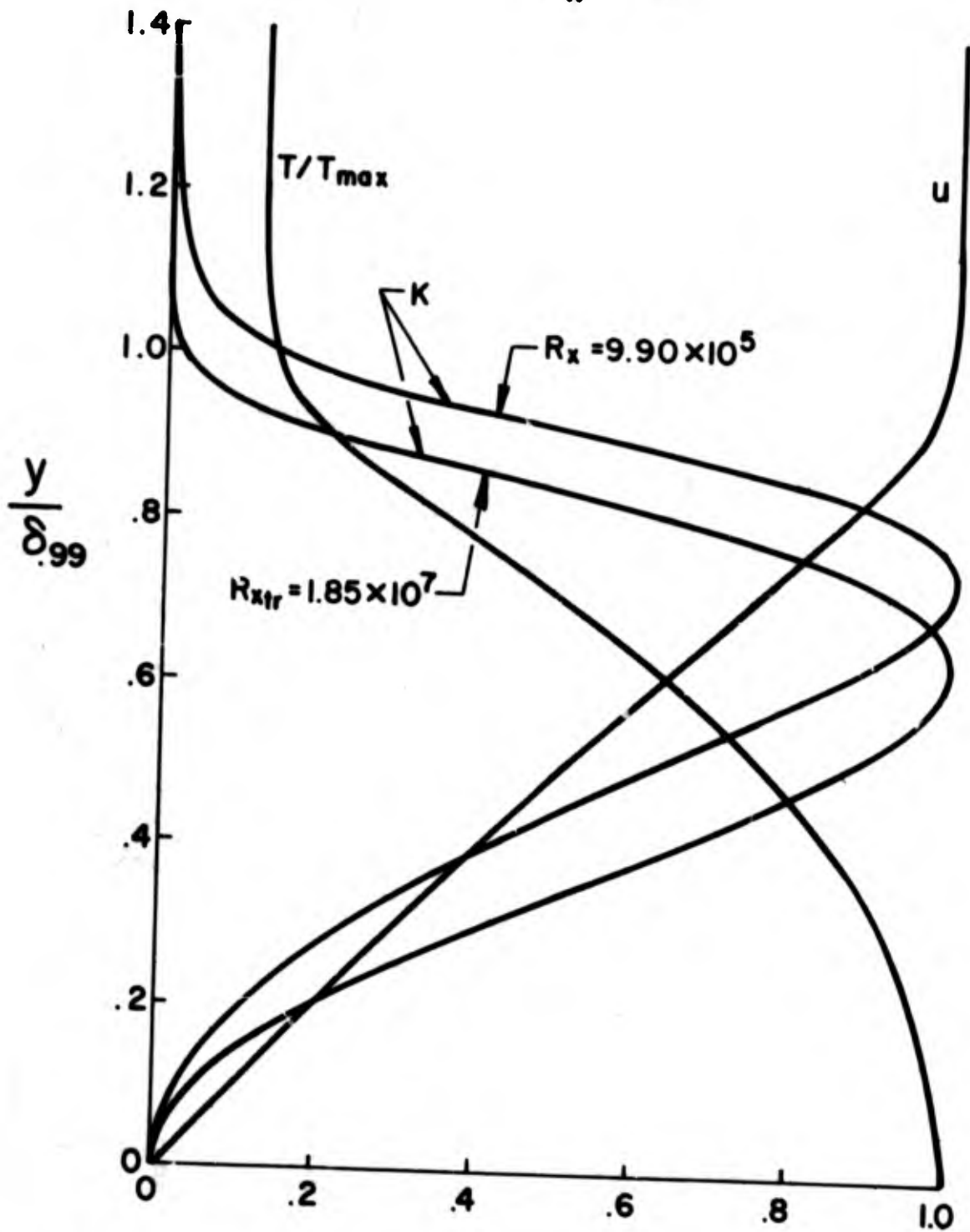


Figure 14. Mean velocity, temperature and turbulent energy profiles for $M = 6$ and $G_w = 1.0$.

M=12.0
G_w=1.0

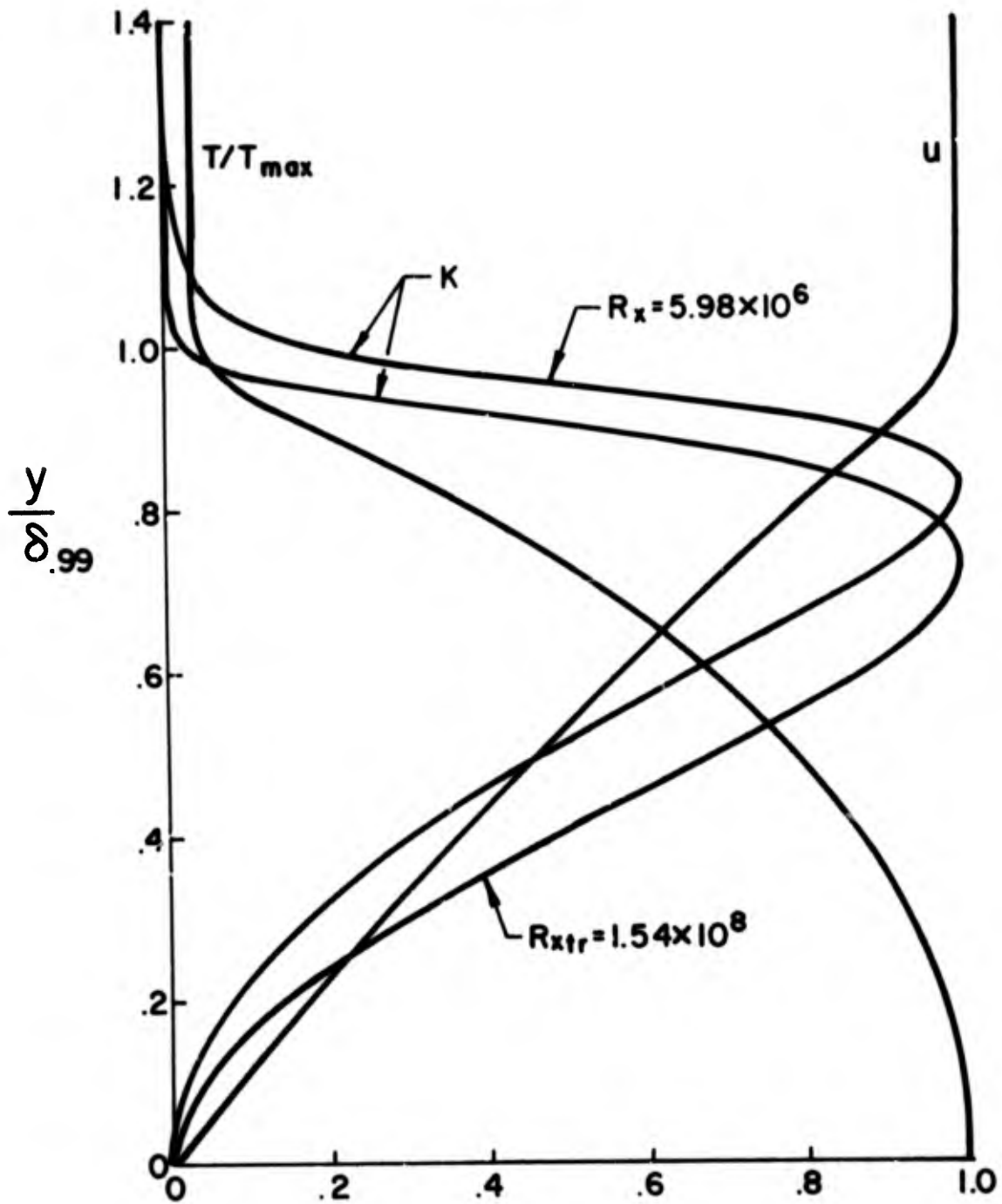


Figure 15. Mean velocity, temperature and turbulent energy profiles for $M = 12$ and $G_w = 1.0$.